



Application of nano adsorbent of PCMC in water treatment : removal of cationic dyes

R.E. Khalifa^a, Moustapha Salem Mansour^a, Ebrahim Esmail Ebrahim^b,
Ibrahim Ashour^b, Mohamed S. Elgeundi^c

^a Chemical Engineering Department Faculty of Engineering Alexandria University

^b Chemical Engineering Department Faculty of Engineering Minia University

^c Polymer Materials Research Department, Institute of Advanced Technology and New Materials, City for Scientific Research and Technological applications, New Borg El-Arab City, Alexandria- Egypt



CrossMark

Abstract

In the present study, modified carboxymethyl cellulose (CMC) was prepared to form nano phosphonate carboxy methyl cellulose (PCMC) for adsorptive removal of cationic dyes methylene blue (MB) and crystal violet as models. The produced nano structure and morphology of the PCMC was investigated by Fourier transform infrared (FT-IR) spectroscopic analyses, Transmission Electron Microscopic (TEM), scanning electron microscopy (SEM) and Zeta potential. Adsorption characteristics of the PCMC for removal of a cationic dyes (MB& CV) were investigated spectrophotometrically as a function of initial dye concentration and contact time, adsorbent dosage, solution pH and temperature. The maximum adsorption capacities of the PCMC nano particles-based on adsorbent for both MB and CV were described by the equilibrium adsorption data of both the dyes which fitted well with Langmuir model ($R^2 = 0.9942, 0.9958$) for dyes respectively. The kinetics of adsorption followed pseudo-first order model. Investigations on thermodynamic parameters in the temperature range of 298–313 K revealed that the adsorption process is spontaneous and endothermic in nature. On the optimized parameter, the adsorbent shows a very high efficiency and rapid removal property for both the dyes.

Keywords: cationic dyes, adsorption, nano particles, carboxy methyl cellulose.

1. Introduction

In recent years, the scientific community around the world has been increasingly concerned about environmental contamination in general, and water pollution in particular.[1] When compared to the overall amount of water available worldwide, the availability of freshwater resources is quite limited.[2] One of these pollutants is Colour pollution, and even a trace amount of colouring material renders it unappealing owing to its look.[3] Synthetic dyes are present in waste water effluents from various industries such as textile, food processing, cosmetics, rubber, and plastics.[4] Dyes are hazardous aromatic compounds with complicated aromatic structures.[5]

Dyes have high resistant to light, air, acids, washing and bases. Because of the high solubility of dyes in water, dyes become one of the most dangerous forms of water pollution.[6] especially, Synthetic dyes which cover a wide range of industrial applications, including the dyeing of silk, leather, paper, wool, and cotton.[7],[8] Methylene blue (MB) has been used as a popular cationic dye model in research. MB easily aggregates and is highly soluble in solutions, which cause Breathing difficulty, eye burn.[9]

In recent decades, a number of biological and physicochemical techniques for the removal of organic dyes and pigments from wastewaters have been published.[10][11] These approaches are grouped into three major categories: physical, chemical, and biological.[11](a)physical (adsorption, filtration, and flotation, flocculation separation, and activated carbon adsorption).[12](b)chemical (conventional advanced oxidation processes such as photo catalysis, ozonation, chlorination[13],reduction, electrochemical), and(c)biological(aerobicand anaerobic degradation).[14]

Among of these techniques, adsorption is one of the most effective one , with a lot of advantages such as low operating costs, and the removal without producing dangerous by-products.[15] Many research groups have investigated dye adsorption including clay, biomass, activated carbon, and zeolites. These are of a limited use due to low adsorption capacity and are high cost. Natural polymers such as starch, cellulose, and chitin are receiving a growing interest. [16][17]

Cellulose is a naturally hygroscopic and hydrophilic substance that can absorb water.[18]The surface of cellulose contain hydroxyl groups, which give it a

*Corresponding author e-mail: hadier.ragab@aiet.edu.eg; (Inst.Hadier Ragab).

Receive Date: 19 November 2022, Revise Date: 29 January 2023, Accept Date: 11 May 2023

DOI: 10.21608/EJCHEM.2023.175693.7207

©2023 National Information and Documentation Center (NIDOC)

hydrophilic character and increase the availability of cellulose surface to be modified.[19] Carboxy methyl cellulose is a cellulose derivative that is produced in the sodium salt form to obtain sodium carboxy methyl cellulose. It is available as a white or milky powder that is tasteless and odorless.[20]

Carboxymethyl cellulose (CMC) has a variety of uses in the food, pharmaceutical, detergent, and coatings industries. It is an anionic linear polymer in which the original H atom in the hydroxyl group of cellulose has been replaced by a carboxymethyl methyl group (-CH₂-COO-).[21] Surface modification caused by physical or chemical method[22] Because of its high stability and hydrophilicity, direct chemical modification of cellulose, such as etherification and esterification, is complex.[23] Surface modification of cellulose can be made by other function group.

The aim of this work to study the effect of modified CMC on the removal of cationic dyes (MB & CV) from water. The adsorption influencing parameters such as initial dye concentration, adsorbent dose, pH, temperature and contact time were optimized for the highest removal of dye from the aqueous solution. The prepared modified CMC was characterized by the Fourier transform infrared (FT-IR) spectroscopic analyses, Transmission Electron Microscopic (TEM), scanning electron microscopy (SEM) and Zeta potential.

2. Materials and methods

2.1. Materials

Sodium Carboxy Methyl Cellulose (CMC) low viscosity (ADWIC, pure lab. Chemicals), Epichlorohydrin (ECH) C₃H₅ClO (LOBA Chemie), Ortho Phosphoric acid H₃PO₄=98 (OPA), Ethanol (made in Germany). The cationic dyes Methylene blue (MB) and Crystal violet (CV) used as standard impurities. The chemical formula, molecular formula, and other properties of both dyes are shown in Table.1[24] Sodium Hydroxide (NaOH) and Hydrochloric acid (HCl) were used for maintaining the pH during batch experiments to study the impact of processing parameters.

Table 1 chemical formula, molecular formula, and other properties of Methylene Blue (MB) and Crystal Violet (CV).

Properties	Methylene Blue (MB)	Crystal Violet (CV)
Chemical Formula	C ₁₆ H ₁₁ CIPN ₃ S	C ₂₅ H ₃₀ CIPN ₃
Molecular Weight	319.85 g/mol	408 g/mol
Melting Point	100-110°C	205°C

2.2. procedure:

To prepare phosphonated carboxy methyl cellulose nano particles mix sodium carboxy methyl cellulose (low viscosity concentration 2%) with 0.5 ml of

epichlorohydrin ECH and stir at room temperature for 2 hours. Add 0.4 ml epichlorohydrin ECH and 1 ml ortho phosphoric acid OPA to the mixture for 1.5 hour. The mixture was refluxed on water bath at 55°C for 1 hour then cooled. The product was washed with ethanol. The solid was filtered and dried at 50°C Cover night. Use ball mill (Planetary Ball Mill PM400, Retsch-Allee 1-5, Germany) to obtain nano size. The final product of PCMC was in the form of powder.

2.3. characterization studies

The chemical structure of the developed adsorbent was investigated using Fourier Transform Infrared Spectroscopy (FTIR, BRUKER, TENSOR 37 spectrometer). Physical properties of adsorbent surfaces of PCMC were characterized by scanning electron microscopy (SEM) (JEOL JSM-6010LV). The changes in the surface morphology for the developed adsorbent was studied by using Transmission Electron Microscopy (TEM) (JEOL JTM-1400), Japan and Zeta potential was measured by using (MALVERN, ZETASIZER, Nano-ZS).

3. Results and discussion

3.1 Fourier Transform Infrared (FT-IR)

The surface functional groups of phosphonates carboxy methyl cellulose was obtained by Fourier Transform Infrared (FTIR) spectroscopy analysis. Fig 1 show the FTIR for CMC and PCMC. For CMC in Fig show the peak at 3432 cm⁻¹ was due to the stretching vibration of -OH groups of cellulose[25]. The peak at 2923 cm⁻¹ is due to C-H stretching. The peak at 1422 cm⁻¹ observed for vibrational motions of -COO- groups. The peak at 1599 cm⁻¹ showed a lower wave number shift which corresponding to C=C bond.[26] By addition of phosphate group a new sharp peak appear at 1019 cm⁻¹ was due to -PO₄ group[27] and decrease in the other peaks at 3361,2906,893 cm⁻¹ for -OH,C-H and C=O group, respectively. And vibration motion at peak 1418-1729 cm⁻¹ for C=C bond.

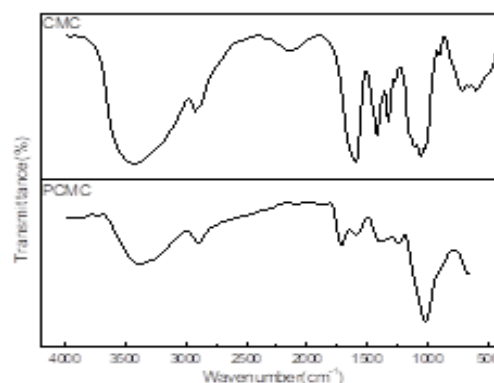


Fig 1 (a) FTIR of CMC, (b) FTIR of PCMC.

3.2 Scanning Electron Microscopy (SEM) analysis

As shown in fig 2 (a) CMC (b) PCMC

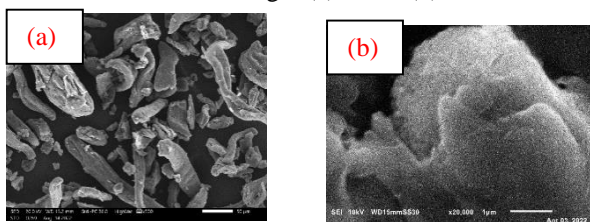


Fig 2 SEM analysis for (a) CMC, (b) PCMC.

3.3 Transmission Electron Microscopy (TEM) analysis

To support the results obtained by SEM analysis, TEM images of PCMC was also recorded. As shown in Fig 3 The particle size around (1.31nm-5.48nm).

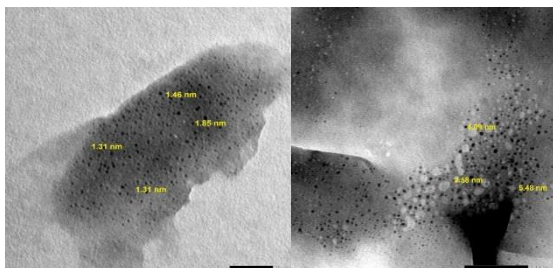


Fig 3 TEM analysis for PCMC.

3.4 Surface characterization of PCMC

Zeta potential of the studied PCMC was measured at pH 7, the zeta potential for the studied PCMC was found to be -21 mV. When the total charge on the surface of adsorbent is zero and zeta potential is zero The pH is measured as point of zero charge (pHPZC).^[1]

3.5 Effect of degree of phosphorization

As shown in Fig 4 the effect of phosphorization on the percentage removal of MB on the surface of PCMC was studied at 298 K and initial concentration 30mg/L, adsorbent dose 0.05g and pH of 7. The results show that the percent removal increase by increasing the degree of phosphorization from 1& 1.5ml phosphoric acid after that the removal decrease with increasing the amount of phosphoric acid.

3.6 Effect of initial dye concentration and contact time

As shown in Fig 5 the effect of initial dye concentration on the percentage removal and dye uptake (qt) of MB and CV was studied at 298 K for adsorbate concentration in the range 10-100 mg /L, adsorbent dose of 0.05 g and solution pH of 7. The results show that the percentage removal of CV & MB dyes decrease by increasing the initial concentration of dyes[24] .The percentage removal decreased from 93.65 to 57.88 in case of MB and from 94.08 to 52.42 in case of CV dye. This may be due to the presence of Large active sites of adsorbent which can attract with

dyes at low concentration but at high concentrations the

3.7 Effect of adsorbent dose

As shown in Fig 6 the effect of adsorbent dose on the percentage removal and dye uptake (qt) of MB and CV was studied by varying the adsorbent amount from 0.05 g/L to 0.08 g L at 298 K, a solution pH of 7 and initial adsorbate concentration of 30 mg/L. The results show that at first removal of MB & CV increased with increasing the adsorbent dosage but at high dosage of adsorbent the percentage or removal slowly increased which indicated that adsorption equilibrium of dye was reached[28].

3.8 Effect of temperature

The temperature is one of the most important factors to determine the process of adsorption. The effect of temperature on adsorption of MB and CV onto PCMC was investigated at (298,303 and 318 K), initial dye concentration 30 mg/L, adsorbent dose 0.05 g and solution pH of 7. As shown in Fig 7 The adsorbed quantity of MB & CV increased by increasing the temperature. This is may be due to increase in the diffusion of dyes molecules by increasing the temperature and generation of active sites on the adsorbent surface but after specific temperature a slightly increase in the percentage of removal may be due to saturation of adsorbent surface with MB & CV molecules.[9]

3.10 Effect of pH

The pH of the solution is one of the important parameters which affect the whole adsorption process. The effect of solution pH on the removal of MB and CV dyes from the aqueous solution was studied for the pH ranging from (3 to 11) using 0.05g adsorbent PCMC, initial concentration 30 mg/L and temperature 298 K. As shown in Fig 8 at first the removal of MB&CV increases with an increase in the pH and after that the increase in pH show a decreasing trend.[29] In case of acidic solution the excess concentrations of H⁺ ions decrease the adsorption between cationic dye on the surface of nano particle adsorbent.[24] At high pH value, the concentration of OH⁻ ions increase in the solution. The cationic dyes react with the OH⁻ ions in the solution to form complex instead of adsorption on the surface of the nano particle adsorbent which cause drop in adsorption efficiency. [30]

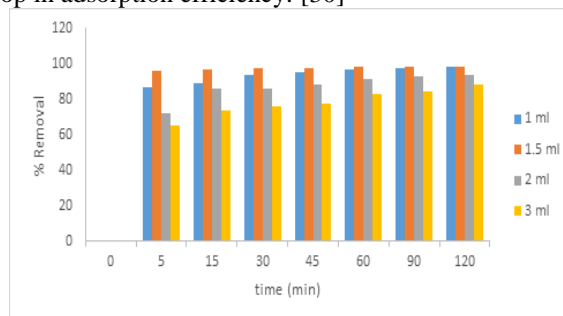


Fig 4Effect of degree of phosphorization on MB removal.

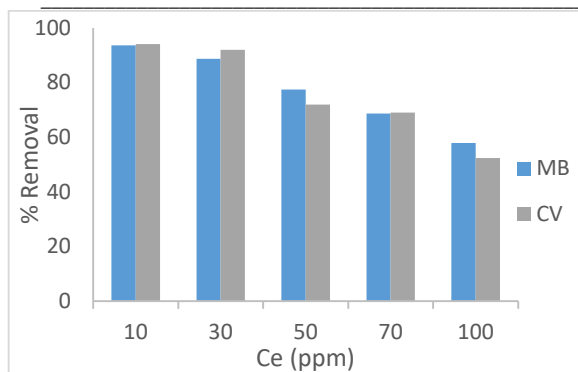


Fig 5 Effect of initial concentration (C_e) and contact time on the removal of MB & CV.

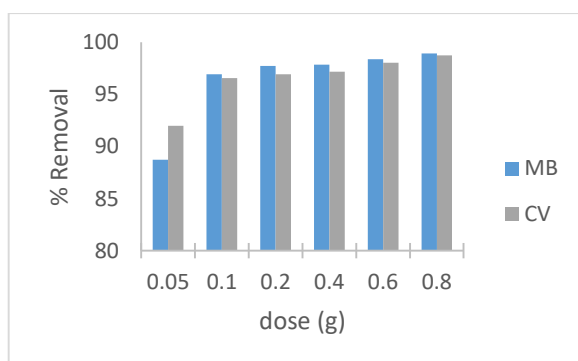


Fig 6 Effect of adsorbent dose on the removal of MB & CV.

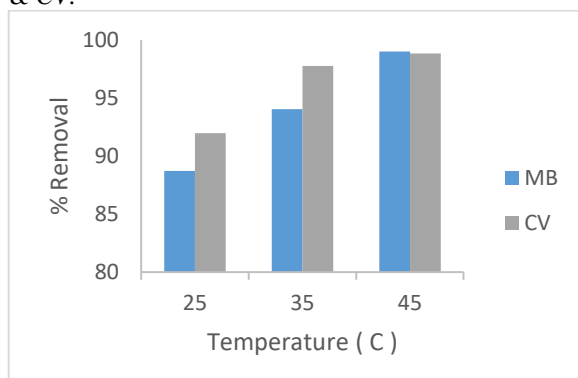


Fig 7 Effect of temperature on the removal of MB & CV.

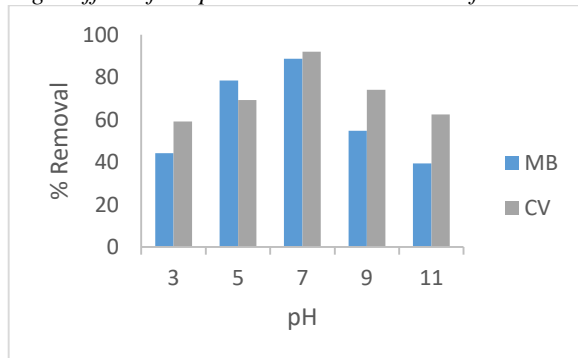


Fig 8 Effect of pH on removal of MB & CV.

4. Equilibrium isotherms

Using the batch process to evaluate the effect of parameters on the amount of dye adsorbed at equilibrium, q_e (mg/g), such as the effect of initial concentration of dye, contact time, pH and temperature. To determine the residual concentration of the dye sample solution was withdrawn at certain time. By using UV-V spectrophotometer at λ of 664 nm[31] and 590 nm[32] for MB & CV respectively.

Adsorption performance was determined by (q_t) using the following equations:

$$q_t = \frac{(C_0 - C_t) * V}{m} \quad (1)$$

$$q_e = \frac{(C_0 - C_e) * V}{m} \quad (2)$$

Where q_t (adsorbed dye per gram of adsorbent at time t mg/g) and q_e (equilibrium adsorption capacity mg/g) and C_t , C_0 , C_e , V , and m represent the concentration at time t (mg/l), the initial concentration (mg/l), the equilibrium concentration, volume of solution (mL) and the mass of adsorbent (g), respectively.[31]

The removal percentage of adsorption was calculated by the following equation[33].

$$\% \text{removal of dye} = \left[\frac{(C_0 - C_t)}{C_0} \right] * 100 \quad (3)$$

4.1 Adsorption Isotherm

Adsorption isotherms, method used to calculate the amount of solute adsorbed per unit of adsorbent, as a function of equilibrium concentration at constant temperature.[33] Five adsorption isotherms are mostly wide used to adjudged the correlation coefficient, R^2 values (Langmuir, Freundlich, Temkin, Dubinin-Radushkevich and Elovich).[30]

4.1.1 Langmuir isotherm

Langmuir adsorption isotherm model, shows that the adsorption usually occurs with numerous monolayer processes[30] non-linear form and the linear form Equation(4) and equation (5) [33] as given :

$$q_e = \frac{q_m K_L C_e}{1 + K_L C_e} \quad (4)$$

$$\frac{1}{q_e} = \frac{1}{K_L q_m C_e} + \frac{1}{q_m} \quad (5)$$

$$\text{And } R_L = \frac{1}{1 + K_L C_0} \quad (6)$$

Where C_e is the equilibrium concentration, mg/L; q_e is the adsorption capacity at equilibrium, mg/g; q_m is maximum adsorption capacity mg/g; K_L is the Langmuir constant, L/mg; R_L is the separation factor obtained from eqn (6). R_L indicates the favourability of the adsorption process. $0 < R_L < 1$ for adsorption is favors, $R_L > 1$ for adsorption is unfavourable, $R_L = 1$ for linear and $R_L = 0$ for reversible.[24] A plot of $1/q_e$ against $1/C_e$ gives a straight line with slope of $1/K_L q_m$ and intercepts $1/q_m$ and correlation coefficient $R^2 = 0.9942$ & 0.9958 as shown in Fig.9 (a) ,10(a) for MB & CV respectively .The data listed in Table(2,3) Which revealed that the q_{max} value is ($62.11 \text{ mg} \cdot \text{g}^{-1}$, $48.3 \text{ mg} \cdot \text{g}^{-1}$) and K_L equal ($0.2009 \text{ L} \cdot \text{mg}^{-1}$, $0.415 \text{ L} \cdot \text{mg}^{-1}$). The lower R_L values for all different

concentrations (10-100 mg/l) for MB between (0.42 - 0.046 mg/l) and R_L values of CV between (0.186 - 0.0248) reflects that adsorption is more favorable and deduce that a mono layer formation is taking place during the adsorption of MB&CV over the surface of PCMC.

4.1.2 Freundlich isotherm

Freundlich isotherm model indicate that the adsorption process takes place in multilayer [24] and shows the heterogeneity of adsorbent surface[28].The nonlinear and linear equation as follow[34]

$$q_e = K_F C_e^{1/n} \quad (7)$$

$$\log(q_e) = \log K_F + \frac{1}{n} \log(C_e) \quad (8)$$

Where C_e is the equilibrium concentration, mg/L; q_e is the adsorption capacity at equilibrium, mg/g; K_F is the Freundlich constant; n is the intensity of adsorption. As shown in Fig.9 (b), 10(b) by plotting $\log q_e$ versus $\log C_e$ the slope and intercept can be calculated. K_F gives indication about the bonding energy and/or distribution coefficient and represents the quantity of dye adsorbed onto an adsorbent. $1/n$ shows adsorption intensity that takes value ranges between 0 and 1. When the value of $1/n$ is equal to 1, the adsorption is linear, while the value of $1/n < 1$ indicates the chemically driven adsorption process and the value of $1/n > 1$ indicates the physical adsorption. [32] The values of $1/n$ (0.35,0.26) for MB, CV give an indication of the favorability of adsorption and high tendency of MB and CV for the adsorption onto PCMC. All parameters are listed in Table (2,3).

4.1.3 Temkin isotherm

This model used to determine the heat of adsorption (adsorbent-adsorbate interaction) over the surface of PCMC applied at room temperature which represented by the Equation (9) [33]

$$q_e = B \ln A_T + B \ln C_e \quad (9)$$

Where

$$B = RT/b \quad (10)$$

In this model B is the heat of adsorption ($J \text{ mol}^{-1}$); A_T (L/g) is the equilibrium binding energy for Temkin model. By plotting q_e against $(\ln C_e)$ as shown in Fig.9 (c), 10 (c) to obtain the slope (B) and intercept ($B \ln A_T$). R the gas constant ($8.314 \text{ J/mol}\cdot\text{K}$), and T is the temperature, the positive value of constant B is ($13.149, 8.9639 \text{ J/mol}$) indicates an endothermic process for MB and CV.[33] The value of the correlation coefficient R^2 (0.9869,0.955) for MB and CV respectively.

4.1.4 Dubinin-Radushkevich isotherm (DKR)

The Dubinin-Kaganer-Radushkevich (DKR) has been used to evaluate the porosity properties of the adsorbent and the energy of adsorption process. The DKR equation has the form [35]

$$\ln q_e = \ln q_D - 2B_D RT \ln(1 + 1/C_e) \quad (11)$$

And

$$E_{D-R} = \sqrt{1/2 B_D} \quad (12)$$

Where R , is the gas constant ($0.08314 \text{ KJ/mol}\cdot\text{K}$); T absolute temperature (K); q_D and B_D are the constants of Dubinin-Radushkevich model obtained from slope and intercept of plotting $(\ln q_e)$ against $(\ln(1+1/C_e))$ as shown in Fig.9 (d), 10 (d). The value of E_{D-R} , Table (2,3) gives information about the type of adsorption mechanism as chemical or physical adsorption. The value of E_D equal ($0.495, 0.2527 \text{ kJ/mol}$) suggested that mechanism of adsorption process chemical adsorption of dye molecule.[33]

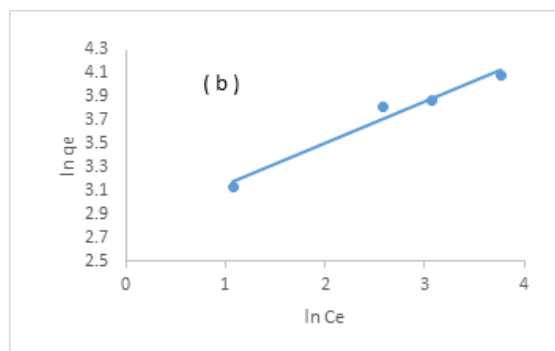
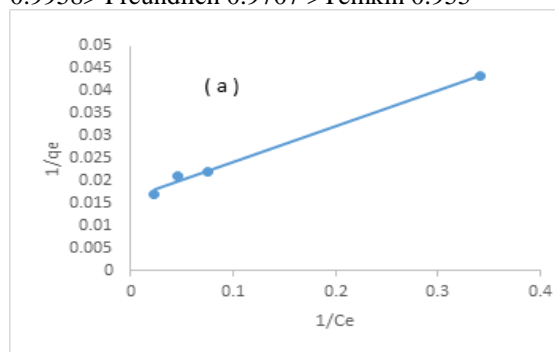
4.1.5 Elovich isotherm

Elovich model describes the adsorption process by the equation:

$$\ln \frac{q_e}{C_e} = \ln(K_E q_m) - \frac{1}{q_m} q_e \quad (13)$$

Where K_E is equilibrium constant ($L \text{ mg}^{-1}$) q_m is the Elovich maximum adsorption capacity (mg/g) can be calculated from the slopes and the intercepts of the linear plot between $\ln(q_e/C_e)$ vs q_e as shown in Fig 9 (e), 10 (e) give a straight line with the correlation coefficient (0.9626,0.9453) for MB and CV. The calculated parameters from isotherm models are summarized in Table (2,3). For adsorption of MB on the surface of PCMC the values of the regression coefficient (R^2) for Langmuir isotherm close to unity (0.9942).

The correlation coefficient of different adsorption models is lower than other applicable models and the order is Langmuir 0.9942 > Temkin 0.9869 > D-R 0.9777 > Freundlich 0.9696 > Elovich 0.9626 for MB. And for CV adsorption on to PCMC fitted the best into Langmuir isotherm model. The R^2 value for Langmuir 0.9958 > Freundlich 0.9707 > Temkin 0.955



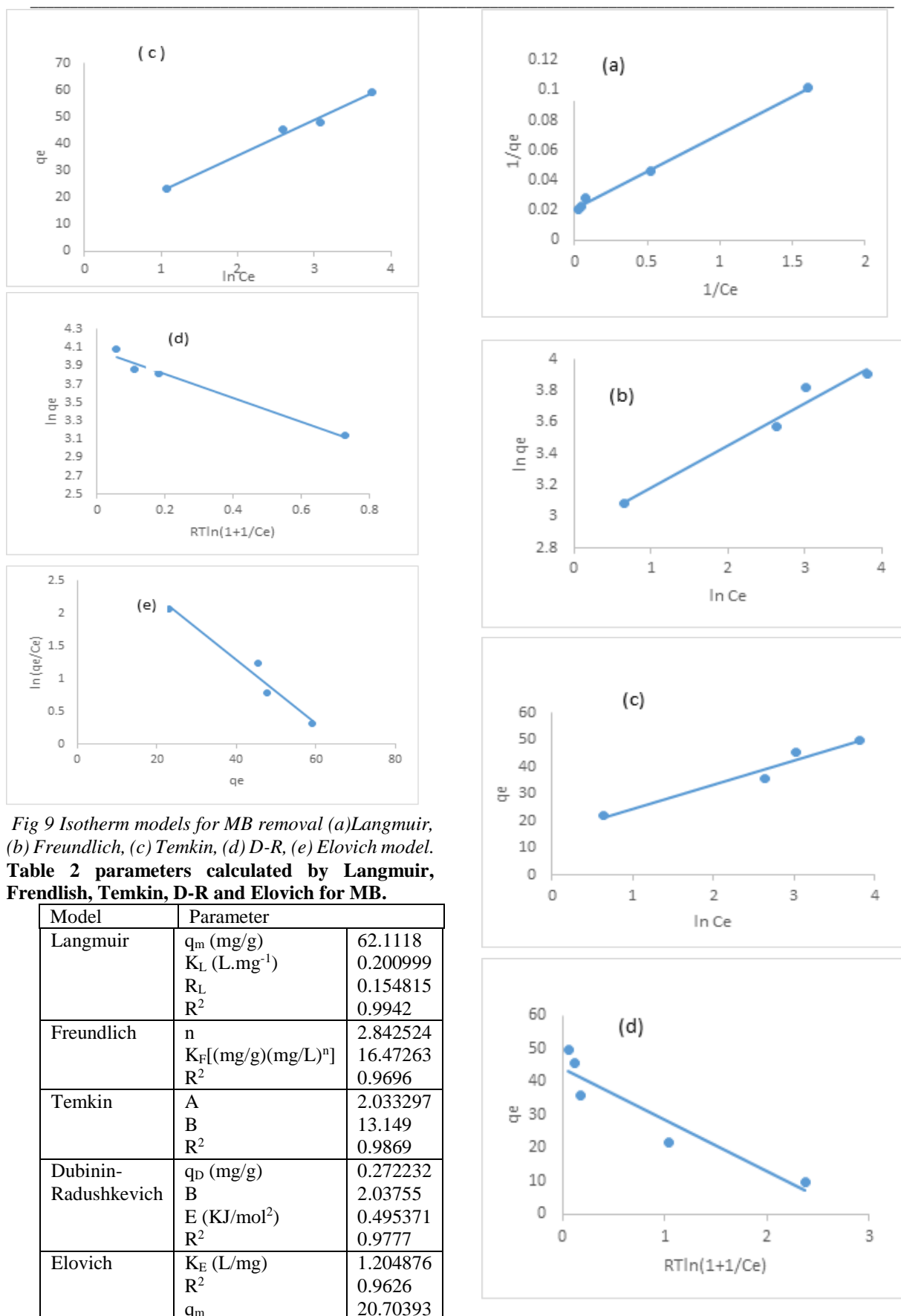


Fig 9 Isotherm models for MB removal (a)Langmuir, (b) Freundlich, (c) Temkin, (d) D-R, (e) Elovich model.

Table 2 parameters calculated by Langmuir, Freundlich, Temkin, D-R and Elovich for MB.

Model	Parameter	
Langmuir	q_m (mg/g)	62.1118
	K_L (L.mg ⁻¹)	0.200999
	R_L	0.154815
	R^2	0.9942
Freundlich	n	2.842524
	$K_F[(\text{mg/g})(\text{mg/L})^n]$	16.47263
	R^2	0.9696
Temkin	A	2.033297
	B	13.149
	R^2	0.9869
Dubinin-Radushkevich	q_D (mg/g)	0.272232
	B	2.03755
	E (KJ/mol ²)	0.495371
	R^2	0.9777
Elovich	K_E (L/mg)	1.204876
	R^2	0.9626
	q_m	20.70393

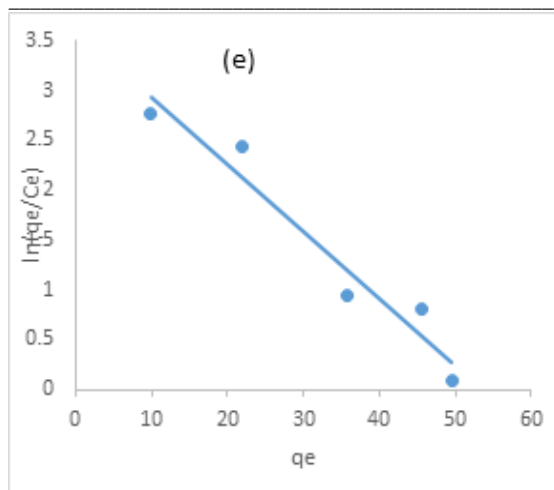


Fig 10 Isotherm models for CV removal (a) Langmuir, (b) Freundlich, (c) Temkin, (d) D-R, (e) Elovich.

Table 3 parameters calculated by Langmuir, Freundlich, Temkin, D-R and Elovich for CV removal by using PCMC.

Model	Parameter	
Langmuir	q_m (mg/g)	48.30918
	K_L (L.mg ⁻¹)	0.415663
	R_L	0.076959411
	R^2	0.9958
Freundlich	n	3.709199
	$K_F[(\text{mg/g})(\text{mg/L})^n]$	18.44512
	J	0.9707
	R^2	
Temkin	A	5.658587
	B	8.9639
	R^2	0.955
Dubinin-Radushkevich	q_D (mg/g)	1.75573E+1
	B	9
	E (KJ/mol ²)	7.8295
	R^2	0.252707
Elovich	K_E (L/mg)	2.42283257
	R^2	0.9453
	q_m	14.9253731

5. Adsorption kinetics

The adsorption kinetics of MB & CV on the surface of PCMC were studied by using pseudo first order, pseudo second order and Elovich models.^[1] The experimental data for the 2 dyes were studied at different initial concentrations and different temperatures. The linear form for pseudo first order represented as follow[36]:

$$\log(q_e - q_t) = \log q_e - \frac{K_1}{2.303} t \quad (14)$$

Where q_e and q_t are the amount of dye adsorbed (mg/g) at equilibrium time t (min). K_1 is rate constant of adsorption (1/min) was calculated from the slope of the plot of $\log(q_e - q_t)$ versus t [36] Fig (11,14,17&20)

and the values of kinetic parameter were presented in Table (4).

The linear form of the pseudo-second-order model is represented in equation [37]

$$\frac{t}{q_t} = \frac{1}{K_2 q_e^2} + \frac{t}{q_e} \quad (15)$$

Where K_2 is the equilibrium constant of adsorption and calculated from the intercept of linear relation between t/q_t and t as shown in Fig (12,15,18 &21) and q_e obtained from the slope. The kinetic parameters were presented in Table 5.

The linear form of Elovich model as follow:

$$q_t = \left(\frac{1}{\beta}\right) \ln(\alpha\beta) + \left(\frac{1}{\beta}\right) \ln t \quad (16)$$

Where α is the initial adsorption rate (mg g⁻¹ min⁻¹) and β is desorption constant during the experiment. The constants obtained from the slope and intercept of linear plot of q_t vs $\ln t$ as shown in fig (13,16,19&22). the corresponding kinetic parameters are in Table6.

The validity of the kinetic models is obtained by correlation coefficients (R^2) given in Table (4,5,6). R^2 for MB and CV obtained from pseudo first order model were higher than the regression coefficient of pseudo second order and Elovich kinetic models. these results show that the adsorption of MB and CV on the surface of PCMC was well followed by the pseudo-first order reaction.

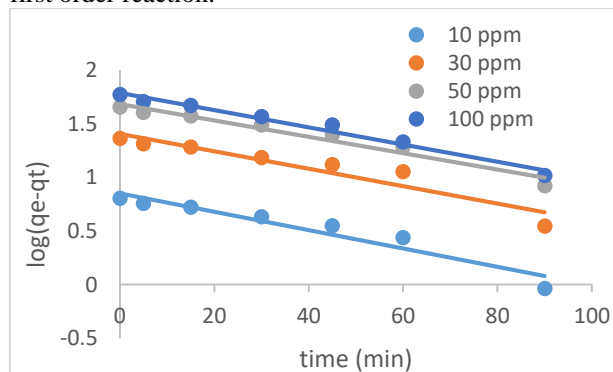


Fig 11 Pseudo first order for MB at different concentrations.

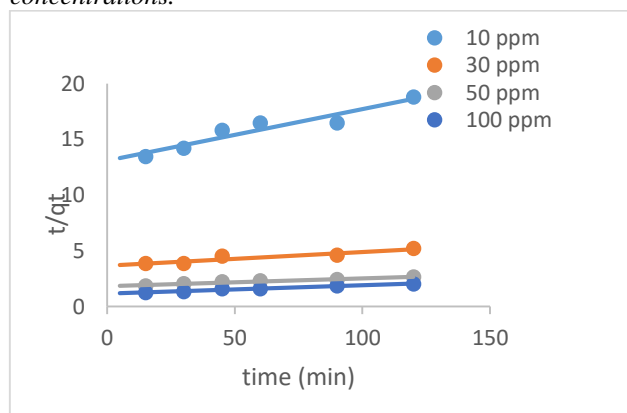


Fig 12 Pseudo second order for MB at different concentrations.

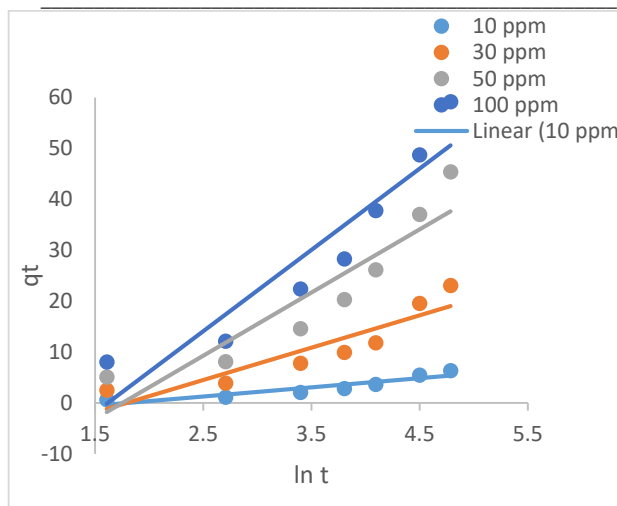


Fig.13. Elovich model for MB at different concentrations

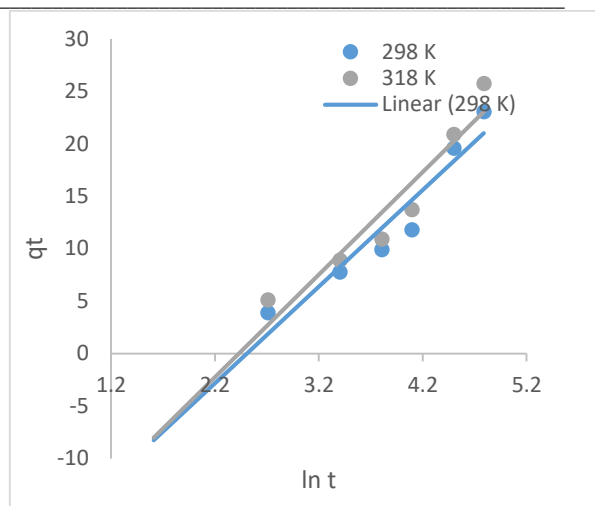


Fig.16. Elovich model for MB at different temperatures.

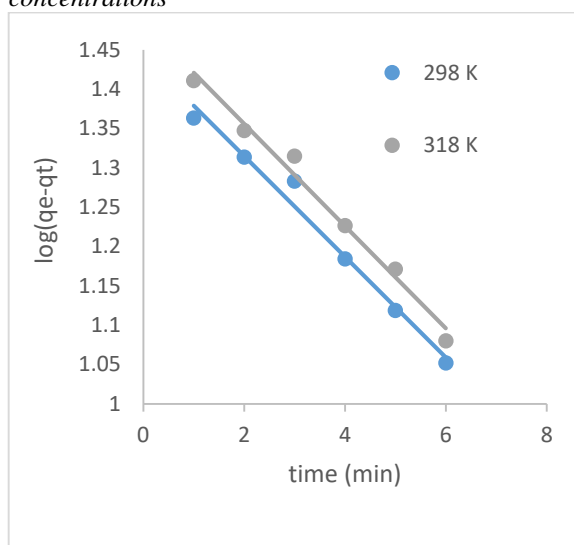


Fig.14. Pseudo first order for MB at different temperatures.

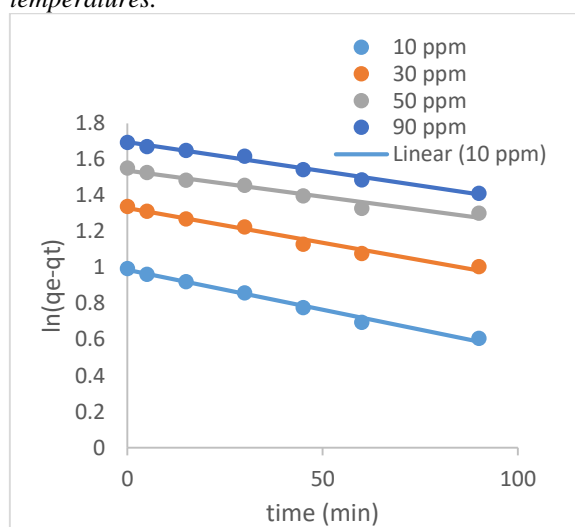


Fig.17. Pseudo first order for CV at different concentrations

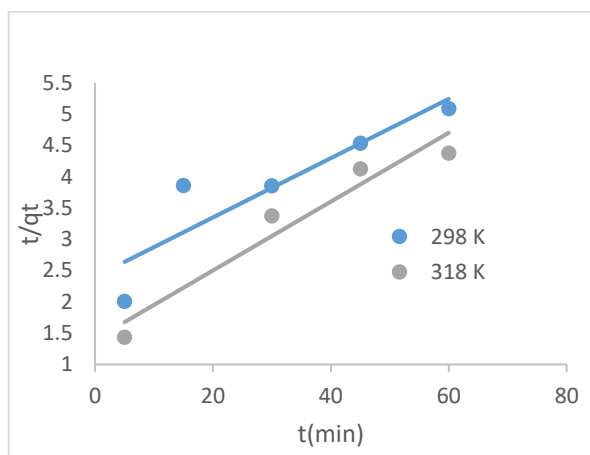


Fig.15. Pseudo second order for MB at different temperatures.

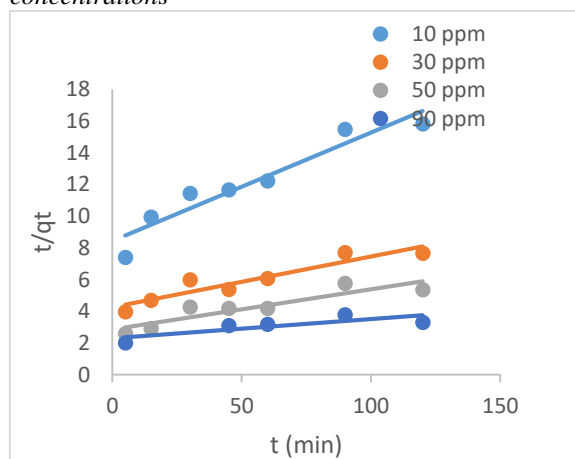


Fig.18. Pseudo second order for CV at different concentrations.

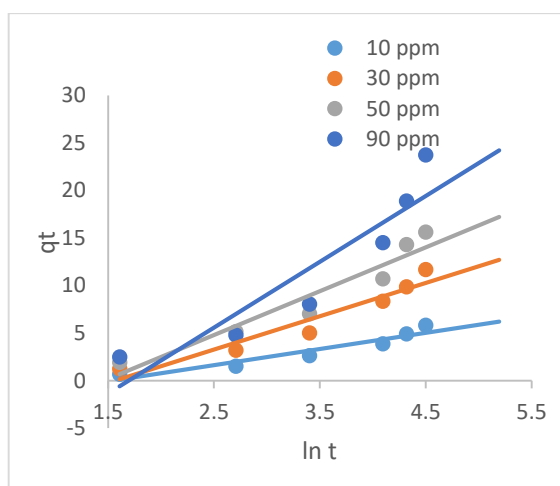


Fig.19. Elovich model for CV at different concentrations.

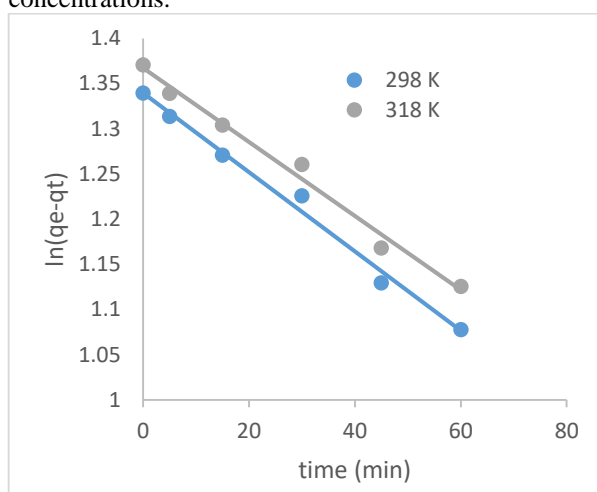


Fig 20 Pseudo first order for CV at different temperatures.

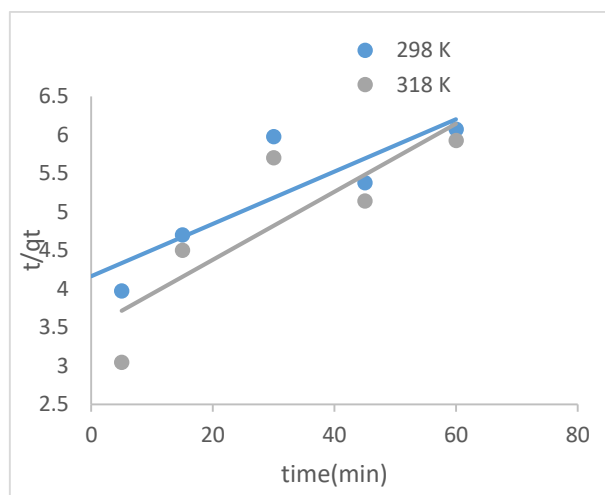


Fig 21 Pseudo second order for CV at different temperatures

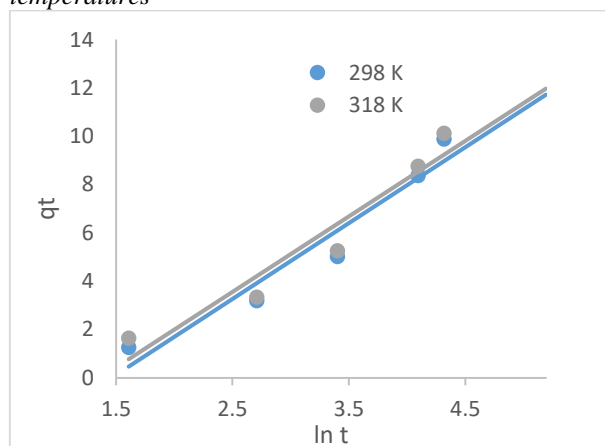


Fig 22 Elovich model for CV at different temperatures

Table 4 Kinetic parameters calculated by Pseudo first order for MB and CV (a) at different initial concentration, (b) at different temperature.

(a) Initial concentration (ppm)	MB			CV		
	K_1 (Lmg ⁻¹)	q_m (mg g ⁻¹)cal	R^2	K_1 (Lmg ⁻¹)	q_m (mg g ⁻¹)cal	R^2
10	0.019806	7.123608	0.9262	0.010133	9.693933	0.9904
30	0.018654	25.55642	0.9008	0.008751	21.35502	0.9796
50	0.017733	48.52885	0.9582	0.006679	34.52232	0.9594
100	0.018424	61.40447	0.9783	0.00737	49.65923	0.9887

(b) Temperature (K)	MB			CV		
	K_1 (Lmg ⁻¹)	q_m (mg g ⁻¹)cal	R^2	K_1 (Lmg ⁻¹)	q_m (mg g ⁻¹)cal	R^2
298	0.147162	27.72682	0.9815	0.010133	21.85244	0.9905
318	0.149465	30.5844	0.9853	0.009442	23.28627	0.9879

Table 5 Kinetic parameters calculated by Pseudo second order for MB and CV (a) at different initial concentration, (b) at different temperature.

(a) Initial concentration (ppm)	MB			CV		
	K_2 (g mg ⁻¹ min ⁻¹)	q_m (mg g ⁻¹)cal	R^2	K_2 (g mg ⁻¹ min ⁻¹)	q_m (mg g ⁻¹)cal	R^2
10	0.000163	21.64502	0.909	0.000554	14.64129	0.9122
30	3.97724E ⁻⁵	82.6446281	0.8717	0.000239	31.34796	0.8828
50	2.68273E ⁻⁵	142.8571429	0.9565	0.000224	39.52569	0.8224
100	4.87646E ⁻⁵	133.3333333	0.9695	6.36482E ⁻⁵	82.6446281	0.6547

(b)Temperature (K)	MB		CV			
	$K_2(\text{g mg}^{-1} \text{min}^{-1})$	$q_m(\text{mg g}^{-1})_{\text{cal}}$	R^2	$K_2(\text{g mg}^{-1} \text{min}^{-1})$	$q_m(\text{mg g}^{-1})_{\text{cal}}$	R^2
298	0.000932	21.14165	0.8176	0.000276	29.49853	0.7215
318	0.002149	18.21494	0.9379	0.000559	22.62443	0.718

Table 6 Kinetic parameters calculated by Elovich model for MB and CV (a) at different initial concentration, (b) at different temperature.

(a)Initial concentration (ppm)	MB			CV		
	$\alpha (\text{mg g}^{-1} \text{min}^{-1})$	$\beta (\text{g mg}^{-1})$	R^2	$\alpha (\text{mg g}^{-1} \text{min}^{-1})$	$\beta (\text{g mg}^{-1})$	R^2
10	0.299588	0.556979	0.8525	0.364568	0.586476	0.9133
30	1.060588781	0.157838247	0.8271	0.733623	0.285111	0.9252
50	2.147264152	0.080528265	0.8492	1.072223	0.216506	0.9197
100	3.158475165	0.062644866	0.8779	1.273747839	0.144483616	0.8507

(b)Temperature (K)	MB			CV		
	$\alpha (\text{mg g}^{-1} \text{min}^{-1})$	$\beta (\text{g mg}^{-1})$	R^2	$\alpha (\text{mg g}^{-1} \text{min}^{-1})$	$\beta (\text{g mg}^{-1})$	R^2
298	0.750769	0.108554	0.9161	0.729569	0.318583	0.9383
318	0.861964	0.102336	0.9108	0.799821	0.319734	0.9298

6. Thermodynamic study

It is used to calculate the temperature effect on the process of adsorption of MB and CV on the surface of PCMC. The thermodynamic parameters are enthalpy (ΔH^0), entropy (ΔS^0) and Gibbs free energy (ΔG^0), are calculated

As follow [36]

$$\Delta G^0 = -RT \ln K_L \quad (17)$$

$$\ln K_L = \frac{\Delta S^0}{R} - \frac{\Delta H^0}{RT} \quad (18)$$

$$\Delta G^0 = \Delta H^0 - T\Delta S^0 \quad (19)$$

Where K_L is (q_e/C_e) the Langmuir constant (L/g), R is the universal gas constant (8.314 J/mol K), and T is the absolute temperature (K). ΔH^0 and ΔS^0 were calculated by plotting $\ln(K_L)$ versus $1/T$ as shown in Fig (23,24). The results are listed in Table (7). The negative value of ΔG^0 give indication about the feasibility and the spontaneous nature of the adsorption.[36]. the values of ΔG^0 is (-4.62022 and -11.5943 kJ/mol) for MB and (-6.28489 and -12.0099 KJ/mol) for CV which suggest that the adsorption process is physisorption.[36]. And indicates that the adsorption of MB and CV onto the PCMC is spontaneous and thermodynamically favorable at all temperatures tested here^[1]

The enthalpy change (ΔH^0) for the adsorption process of MB and CV as calculated were 99.2941 kJ mol⁻¹ and 79.01792 kJ mol⁻¹, respectively. This positive value of ΔH^0 indicates that the process of adsorption is endothermic. The high values of ΔH^0 are may be due to the presence of strong bond between adsorbent and molecules of dyes.^[1] the entropy (ΔS^0) shows positive value which indicates that there was increased randomness during the process of adsorption.[38]

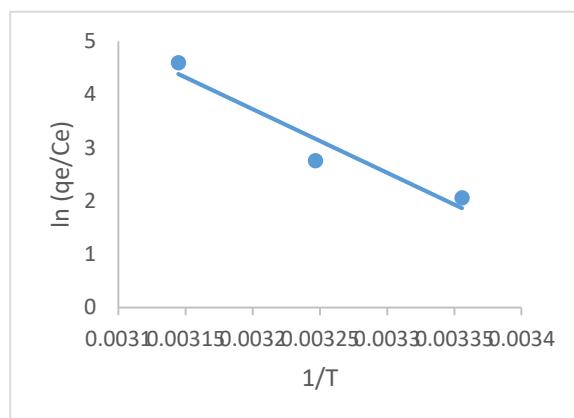


Fig 23 Thermodynamic for MB.

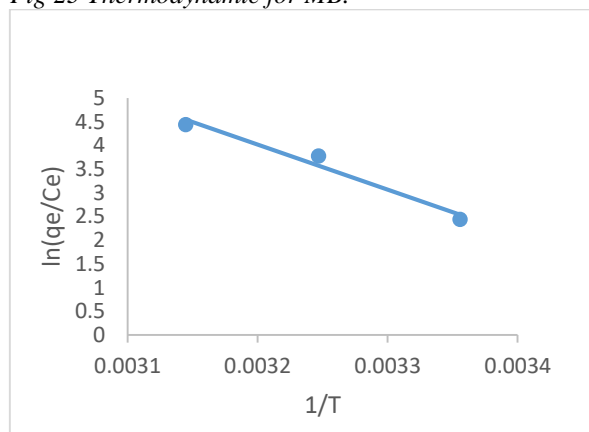


Fig24 Thermodynamic for CV.

Table 7 thermodynamic for MB & CV removal.

Temperatures, K	Van't Hoff Equation					
	ΔG , kJ/mol		ΔH , kJ/mol		ΔS , J/mol·K	
	MB	CV	MB	CV	MB	CV
298	-4.62022	-6.28489	99.2941	79.01792	348.7058	286.251
303	-8.10728	-9.1474				
318	-11.5943	-12.0099				

7. Conclusion

In this study the modified carboxy methyl cellulose (PCMC) used to remove the both cationic dyes methylene blue and crystal violet from aqueous solution at different operating parameters such as amount of adsorbent, pH, contact time and temperature. The PCMC was characterized by the FT-IR, SEM, TEM and zeta potential analyses. The size of the nanoparticles was interpreted using TEM. The operating conditions was studied as follow The %removal was increased by increasing contact time and amount of adsorbent and decreasing the initial concentration of dye but in case of pH the neutral medium is the best removal for the both dyes. The Pseudo first order kinetic model of adsorption was followed. Langmuir isotherm was best fitted with the experimental data confirming monolayer adsorption. The temperature effect was also used to calculate the change in activation enthalpy (ΔH^0), free energy of adsorption (ΔG^0), and entropy (ΔS^0). This fundamental study will be helpful for the technology of removing dyes from wastewater. The thermodynamic parameter change in enthalpy (ΔH^0) shows positive value which indicates that the adsorption process is endothermic. The change in entropy (ΔS^0) shows a positive value indicating an increased randomness during the process of adsorption. The Gibbs free energy change (ΔG^0) shows a negative value which indicates that the adsorption process is spontaneous in nature. Overall, it can be concluded that PCMC was effective for removal of CV and MB dyes from the wastewater.

8. References

- [1] L. Borah, M. Goswami, and P. Phukan, "Adsorption of methylene blue and eosin yellow using porous carbon prepared from tea waste: Adsorption equilibrium, kinetics and thermodynamics study," *J. Environ. Chem. Eng.*, vol. 3, no. 2, pp. 1018–1028, 2015, doi: 10.1016/j.jece.2015.02.013.
- [2] M. Sridevi, C. Nirmala, N. Jawahar, G. Arthi, S. Vallinayagam, and V. K. Sharma, "Role of nanomaterial's as adsorbent for heterogeneous reaction in waste water treatment," *J. Mol. Struct.*, vol. 1241, p. 130596, 2021, doi: 10.1016/j.molstruc.2021.130596.
- [3] K. Porkodi and K. Vasanth Kumar, "Equilibrium, kinetics and mechanism modeling and simulation of basic and acid dyes sorption onto jute fiber carbon: Eosin yellow, malachite green and crystal violet single component systems," *J. Hazard. Mater.*, vol. 143, no. 1–2, pp. 311–327, 2007, doi: 10.1016/j.jhazmat.2006.09.029.
- [4] H. Jayasanth Kumari, P. Krishnamoorthy, T. K. Arumugam, S. Radhakrishnan, and D. Vasudevan, "An efficient removal of crystal violet dye from waste water by adsorption onto TLAC/Chitosan composite: A novel low cost adsorbent," *Int. J. Biol. Macromol.*, vol. 96, pp. 324–333, 2017, doi: 10.1016/j.ijbiomac.2016.11.077.
- [5] A. T., S. K. P., and S. K. K., "Synthesis of nano-sized chitosan blended polyvinyl alcohol for the removal of Eosin Yellow dye from aqueous solution," *J. Water Process Eng.*, vol. 13, pp. 127–136, 2016, doi: 10.1016/j.jwpe.2016.08.003.
- [6] M. El Sayed and R. Al araby, "Methylene Blue Cationic Dye Removal using AA-Am Hydrogel as An Efficient Adsorbent," *Egypt. J. Chem.*, vol. 0, no. 0, pp. 0–0, 2022, doi: 10.21608/ejchem.2022.118700.5344.
- [7] F. Ge, H. Ye, M. M. Li, and B. X. Zhao, "Efficient removal of cationic dyes from aqueous solution by polymer-modified magnetic nanoparticles," *Chem. Eng. J.*, vol. 198–199, pp. 11–17, 2012, doi: 10.1016/j.cej.2012.05.074.
- [8] samar ghonim, A. Amin, M. Shaltout, M. Nassar, and H. Youssef, "Synthesis and Application of Nanoporous Adsorbents based on Natural Resource in Dye Removal from water," *Egypt. J. Chem.*, vol. 0, no. 0, pp. 0–0, 2022, doi: 10.21608/ejchem.2022.114237.5195.
- [9] C. Liu, A. M. Omer, and X. kun Ouyang, "Adsorptive removal of cationic methylene blue dye using carboxymethyl cellulose/k-carrageenan/activated montmorillonite composite beads: Isotherm and kinetic studies," *Int. J. Biol. Macromol.*, vol. 106, pp. 823–833, 2018, doi: 10.1016/j.ijbiomac.2017.08.084.
- [10] Z. Yang *et al.*, "Flocculation of both anionic and cationic dyes in aqueous solutions by the amphoteric grafting flocculant carboxymethyl chitosan-graft-polyacrylamide," *J. Hazard. Mater.*, vol. 254–255, no. 1, pp. 36–45, 2013, doi: 10.1016/j.jhazmat.2013.03.053.
- [11] T. Madrakian, A. Afkhami, M. Ahmadi, and H. Bagheri, "Removal of some cationic dyes from aqueous solutions using magnetic-modified multi-

- walled carbon nanotubes,” *J. Hazard. Mater.*, vol. 196, pp. 109–114, 2011, doi: 10.1016/j.jhazmat.2011.08.078.
- [12] R. Gong, M. Li, C. Yang, Y. Sun, and J. Chen, “Removal of cationic dyes from aqueous solution by adsorption on peanut hull,” *J. Hazard. Mater.*, vol. 121, no. 1–3, pp. 247–250, 2005, doi: 10.1016/j.jhazmat.2005.01.029.
- [13] B. Bethi, S. H. Sonawane, I. Potoroko, B. A. Bhanvase, and S. S. Sonawane, “Novel hybrid system based on hydrodynamic cavitation for treatment of dye waste water: A first report on bench scale study,” *J. Environ. Chem. Eng.*, vol. 5, no. 2, pp. 1874–1884, 2017, doi: 10.1016/j.jece.2017.03.026.
- [14] A. Afkhami, M. Saber-Tehrani, and H. Bagheri, “Modified maghemite nanoparticles as an efficient adsorbent for removing some cationic dyes from aqueous solution,” *Desalination*, vol. 263, no. 1–3, pp. 240–248, 2010, doi: 10.1016/j.desal.2010.06.065.
- [15] Y. Wang, Y. Yu, H. Li, and C. Shen, “Comparison study of phosphorus adsorption on different waste solids: Fly ash, red mud and ferric-alum water treatment residues,” *J. Environ. Sci. (China)*, vol. 50, pp. 79–86, 2016, doi: 10.1016/j.jes.2016.04.025.
- [16] H. Yan, H. Li, H. Yang, A. Li, and R. Cheng, “Removal of various cationic dyes from aqueous solutions using a kind of fully biodegradable magnetic composite microsphere,” *Chem. Eng. J.*, vol. 223, pp. 402–411, 2013, doi: 10.1016/j.cej.2013.02.113.
- [17] S. Kamal *et al.*, “Synthesis, characterization and DFT studies of water stable Cd(II) metal-organic clusters with better adsorption property towards the organic pollutant in waste water,” *Inorganica Chim. Acta*, vol. 512, no. July, p. 119872, 2020, doi: 10.1016/j.ica.2020.119872.
- [18] D. W. Wei, H. Wei, A. C. Gauthier, J. Song, Y. Jin, and H. Xiao, “Superhydrophobic modification of cellulose and cotton textiles: Methodologies and applications,” *J. Bioresour. Bioprod.*, vol. 5, no. 1, pp. 1–15, 2020, doi: 10.1016/j.jobab.2020.03.001.
- [19] A. Oberlintner, B. Likozar, and U. Novak, “Hydrophobic functionalization reactions of structured cellulose nanomaterials: Mechanisms, kinetics and in silico multi-scale models,” *Carbohydr. Polym.*, vol. 259, no. February, 2021, doi: 10.1016/j.carbpol.2021.117742.
- [20] A. O. Aliu, J. Guo, S. Wang, and X. Zhao, “Hydraulic fracture fluid for gas reservoirs in petroleum engineering applications using sodium carboxy methyl cellulose as gelling agent,” *J. Nat. Gas Sci. Eng.*, vol. 32, pp. 491–500, 2016, doi: 10.1016/j.jngse.2016.03.064.
- [21] T. Shui *et al.*, “Synthesis of sodium carboxymethyl cellulose using bleached crude cellulose fractionated from cornstalk,” *Biomass and Bioenergy*, vol. 105, pp. 51–58, 2017, doi: 10.1016/j.biombioe.2017.06.016.
- [22] H. M. Ahsan, X. Zhang, Y. Li, B. Li, and S. Liu, “Surface modification of microcrystalline cellulose: Physicochemical characterization and applications in the Stabilization of Pickering emulsions,” *Int. J. Biol. Macromol.*, vol. 132, pp. 1176–1184, 2019, doi: 10.1016/j.ijbiomac.2019.04.051.
- [23] K. Junka, I. Filpponen, L. S. Johansson, E. Kontturi, O. J. Rojas, and J. Laine, “A method for the heterogeneous modification of nanofibrillar cellulose in aqueous media,” *Carbohydr. Polym.*, vol. 100, pp. 107–115, 2014, doi: 10.1016/j.carbpol.2012.11.063.
- [24] S. Rani and S. Chaudhary, “Adsorption of methylene blue and crystal violet dye from waste water using Citrus limetta peel as an adsorbent,” *Mater. Today Proc.*, no. xxxx, pp. 1–9, 2022, doi: 10.1016/j.matpr.2022.01.237.
- [25] H. Li, H. Shi, Y. He, X. Fei, and L. Peng, “Preparation and characterization of carboxymethyl cellulose-based composite films reinforced by cellulose nanocrystals derived from pea hull waste for food packaging applications,” *Int. J. Biol. Macromol.*, vol. 164, pp. 4104–4112, 2020, doi: 10.1016/j.ijbiomac.2020.09.010.
- [26] A. S. Eltaweil, G. S. Elgarhy, G. M. El-Subruiti, and A. M. Omer, “Carboxymethyl cellulose/carboxylated graphene oxide composite microbeads for efficient adsorption of cationic methylene blue dye,” *Int. J. Biol. Macromol.*, vol. 154, pp. 307–318, 2020, doi: 10.1016/j.ijbiomac.2020.03.122.
- [27] A. A. Ahmed, S. Gypser, P. Leinweber, D. Freese, and O. Kühn, “Infrared spectroscopic characterization of phosphate binding at the goethite-water interface,” *Phys. Chem. Chem. Phys.*, vol. 21, no. 8, pp. 4421–4434, 2019, doi: 10.1039/c8cp07168c.
- [28] C. Muthukumar, V. M. Sivakumar, and M. Thirumarimurugan, “Adsorption isotherms and kinetic studies of crystal violet dye removal from aqueous solution using surfactant modified magnetic nano-adsorbent,” *J. Taiwan Inst. Chem. Eng.*, vol. 63, pp. 354–362, 2016, doi: 10.1016/j.jtice.2016.03.034.
- [29] S. Patra, E. Roy, R. Madhuri, and P. K. Sharma, “Agar based bimetallic nanoparticles as high-performance renewable adsorbent for removal and degradation of cationic organic dyes,” *J. Ind. Eng. Chem.*, vol. 33, pp. 226–238, 2016, doi: 10.1016/j.jiec.2015.10.008.
- [30] S. Sultana *et al.*, “Adsorption of crystal violet

- dye by coconut husk powder: Isotherm, kinetics and thermodynamics perspectives,” *Environ. Nanotechnology, Monit. Manag.*, vol. 17, no. January, p. 100651, 2022, doi: 10.1016/j.enmm.2022.100651.
- [31] V. Javanbakht and Z. Rafiee, “Fibrous polyester sponge modified with carboxymethyl cellulose and Zeolitic imidazolate frameworks for methylene blue dye removal in batch and continuous adsorption processes,” *J. Mol. Struct.*, vol. 1249, p. 131552, 2022, doi: 10.1016/j.molstruc.2021.131552.
- [32] F. Shojaeipoor, B. Masoumi, M. H. Banakar, and J. Rastegar, “Aminopropyl-containing ionic liquid based organosilica as a novel and efficient adsorbent for removal of crystal violet from wastewaters,” *Chinese J. Chem. Eng.*, vol. 25, no. 9, pp. 1294–1302, 2017, doi: 10.1016/j.cjche.2016.09.003.
- [33] M. S. Thabet and A. M. Ismaiel, “Sol-Gel γ -Al₂O₃ Nanoparticles Assessment of the Removal of Eosin Yellow Using: Adsorption, Kinetic and Thermodynamic Parameters,” *J. Encapsulation Adsorpt. Sci.*, vol. 06, no. 03, pp. 70–90, 2016, doi: 10.4236/jeas.2016.63007.
- [34] S. M. Abobakr and N. I. Abdo, “Adsorption Studies on Chromium Ion Removal from Aqueous Solution Using Magnetite Nanoparticles,” *Egypt. J. Chem.*, vol. 65, no. 8, pp. 21–29, 2022, doi: 10.21608/ejchem.2022.95319.4475.
- [35] I. Mobasherpour, E. Salahi, and M. Pazouki, “Removal of divalent cadmium cations by means of synthetic nano crystallite hydroxyapatite,” *Desalination*, vol. 266, no. 1–3, pp. 142–148, 2011, doi: 10.1016/j.desal.2010.08.016.
- [36] T. Liu *et al.*, “Adsorption of methylene blue from aqueous solution by graphene,” *Colloids Surfaces B Biointerfaces*, vol. 90, no. 1, pp. 197–203, 2012, doi: 10.1016/j.colsurfb.2011.10.019.
- [37] S. M. Hafez, A. M. Hassan, R. M. El-Shahat, and M. A. Kassem, “Accumulation of Iron, Zinc and Lead by *Azolla pinnata* and Lemna minor and activity in contaminated water,” *Egypt. J. Chem.*, vol. 64, no. 9, pp. 5017–5030, 2021, doi: 10.21608/ejchem.2021.50016.3036.
- [38] S. R. Shirsath, A. P. Patil, B. A. Bhanvase, and S. H. Sonawane, “Ultrasonically prepared poly(acrylamide)-kaolin composite hydrogel for removal of crystal violet dye from wastewater,” *J. Environ. Chem. Eng.*, vol. 3, no. 2, pp. 1152–1162, 2015, doi: 10.1016/j.jece.2015.04.016.